Structural Engineering and Mechanics, *Vol. 66, No. 4 (2018) 445-452*
DOI: https://doi.org/10.12989/sem.2018.66.4.445

Investigation of the model scale and particle size effects on the point load index and tensile strength of concrete using particle flow code

Hadi Haeri*[1], Vahab Sarfarazi[2], Zheming Zhu**[1], Ahmadreza Hedayat[3] and Mohammad Fatehi Marji[4]

[1]*College of Architecture and Environment, Sichuan University, Chengdu 610065, China*
[2]*Department of Mining Engineering, Hamedan University of Technology, Hamedan, Iran*
[3]*Department of Civil and Environmental Engineering, Colorado School of Mines, Golden, CO 80401, United States*
[4]*Department of Mining Engineering, Yazd University, Yazd, Iran*

(Received October 4, 2017, Revised February 26, 2018, Accepted February 28, 2018)

Abstract. In this paper the effects of particle size and model scale of concrete have been investigated on point load index, tensile strength, and the failure processes using a PFC2D numerical modeling study. Circular and semi-circular specimens of concrete were numerically modeled using the same particle size, 0.27 mm, but with different model diameters of 75 mm, 54 mm, 25 mm, and 12.5 mm. In addition, circular and semi-circular models with the diameter of 27 mm and particle sizes of 0.27 mm, 0.47 mm, 0.67 mm, 0.87 mm, 1.07 mm, and 1.27 mm were simulated to determine whether they can match the experimental observations from point load and Brazilian tests. The numerical modeling results show that the failure patterns are influenced by the model scale and particle size, as expected. Both Is(50) and Brazilian tensile strength values increased as the model diameter and particle sizes increased. The ratio of Brazilian tensile strength to Is(50) showed a reduction as the particle size increased but did not change with the increase in the model scale.

Keywords: model scale; particle size; point load test; Brazilian test; PFC2D

1. Introduction

Concrete is a versatile construction material used in many engineering structures. The design of concrete structures requires a thorough understanding of their material properties under various loading conditions. Several experimental investigations have been carried out to examine the behavior of concrete (Silling 2000, Zhou *et al.* 2012, Yang 2015, Zhou *et al.* 2015, Haeri *et al.* 2015a, 2015b, Zhou *et al.* 2015, Li *et al.* 2015, Li *et al.* 2016, Li *et al.* 2016, Haeri and Sarfarazi 2016, Haeri *et al.* 2016, Sarfarazi *et al.* 2016a, Sarfarazi *et al.* 2016b, Bi *et al*. 2016, Sardemir 2016, Shuraim 2016, Haeri *et al*. 2016, Shaowei *et al*. 2016, Wang *et al.* 2017, Bi *et al*. 2017, Haeri *et al.* 2013, 2015, Haeri 2016). The correlation between the strength of concrete and their geometrical dimensions is known as the size effect. The size effects introduce a challenge for scaling up and using the small-scale measured strength data for large-scale applications. To investigate the size effect on strength and fracture energy of concrete, Van Vliet (2000) conducted a series of uniaxial tension experiments to investigate the size effect on the strength and fracture energy of concrete and sandstone. The observed size effect was found to be related to the combination of statistical size effect and strain gradients in the cross section of the specimens (Van Vliet 2000, Vorechovsky 2007). Zi *et al.* (2014) studied the size effect on equi-biaxial flexure strength of concrete by the ASTM C1550 flexure test and the ring-on-ring flexure of circular plates. The four-point flexure test of prismatic beams was also carried out to obtain uniaxial flexural strength for comparison. They observed strong scale dependency in terms of tensile strength, due to the differences in micro-defects and macroscopic cracks. The same factors can also affect the results of numerical simulation efforts using distinct element methods (DEM). DEM allows for fracturing and differential displacements between individual elements. PFC2D, a special DEM code, is based on circular elements and the fundamental laws of contact physics (Cundall 1971, Cundall and Strack 1979, Itasca 1999). Thus, it is an ideal numerical modeling suite for simulating the behaviour of granular materials such as rocks.

To study the behavior of consolidated and well cemented rocks, the PFC2D elements can be modeled as bonded and the bond breakage can be used for evaluation of rock fracturing. The PFC codes have been applied for solving many rock mechanics problems at laboratory scales. Examples include but are not limited to biaxial compression tests of rocks with stress-strain response (Potyondy and Cundall 2004), triaxial testing of rocks with complete stress-strain curves (Aoki 2004, Zhao 2013), evaluation of stresses around an opening (Fakhimi 2002), direct and simple shear testing of rock joints and fault gouges (Cundall 2001, Xu and Ren 2014), acoustic emissions (AE) (Hazzard 2000, 2004) and hydro-fracturing tests of granite (Al-Busaidi 2005) for laboratory scale simulations.

*Corresponding author, Professor
E-mail: haerihadi@gmail.com
**Corresponding author, Professor
E-mail: zhemingzhu@hotmail.com

http://www.techno-press.com/journals/sem&subpage=7
ISSN: 1225-4568 (Print), 1598-6217 (Online)

In addition, PFC has been used to simulate large field scale rock engineering problems such as tunnel excavation and evaluation of EDZ (Aoki 2004), tunnel face stability (Okabe 2004, Yi *et al.* 2014), design of tunnel lining (Tannant 2004), rock cutting and slope stability analysis (Wang 2003), crown pillar's stability (Sainsbury *et al.* 2003), nonlinear dynamical processes (friction and fracture) associated with earthquake (Mora and Place 1998, Morgan and Boettcher 1999), seismic events and the short-time response of adjacent rocks (Mora and Place 1993, Scott 1996, Dalguer *et al.* 2003), large-scale kinematics of geodynamic processes (Erickson *et al.* 2001, Burbidge and Braun 2002, Strayer and Suppe 2002, Vietor 2003), and rock mass with non-persistent joints (Park *et al.* 2004, Ghazvinian *et al.* 2012, Scholtès and Donzé 2012, Bahaaddini *et al.* 2013b, Fan *et al.*, 2015). The development of the smooth joint contact model (SJM) (e.g., Bahaaddini *et al.* 2014, 2013a, 2013b, Chiu *et al.* 2013, Esmaieli *et al.* 2010, Hadjigeorgiou *et al.* 2009, Lambert and Coll 2014, Mas Ivars *et al*. 2011) provided a breakthrough in modeling of discontinuities. The SJM model allows for particles to slide past one another without the need for over-riding each other.

The investigation of the effects of model scale and particle size on tensile strength, point load index and failure processes of numerical models are important to justify the suitability of DEM in modeling of these experiments and the applicability of the numerical modelling results. In this paper, various models with different scales and sizes are studied using PFC2D for both point load test and Brazilian test geometries. The effects of model scale and particle size are obvious on the failure pattern of models, point load index and Brazilian tensile strength.

2. Introduction to PFC2D and its features

PFC2D is a distinct element method program to model mechanical problems that are related to the movement of disc particles. It is also possible to create particles with different shapes such that each group of particles acts as an autonomous object. The particle assembly is created at a uniform size-distribution with radii in the range of the minimum radius to maximum radius. Interactions of discs in an assembly and their response to applied forces, are computed by a finite-difference approach (Itasca 1999) using a large number of individual calculation cycles. During each of cycles, the current contacts between discs are first detected and then a force-displacement law is applied to each of them. Inter-penetration between neighboring discs is controlled by their mechanical micro properties and the applied forces. Micro-properties refer to individual disc contacts and include the parallel or contact bond, normal and shear stiffness components kn and ks, Young's modulus, porosity value, local damping coefficient, size ratio, friction coefficient, and density. The materials used in this study are further characterized by breakable bonds between discs in contact, which bear normal and shear strength as additional micro properties. The Newton's law of motion is used to calculate the resultant disc acceleration (Seyferth and Henk 2006). The circular shape

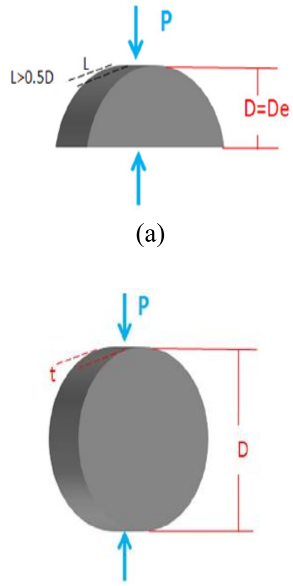

Fig. 1 The schematic view of (a) the point load test and (b) the Brazilian test

and the simple mechanical behavior of PFC2D discs allows for fast and efficient computations and therefore allows for including a large number of elements for a high model resolution (Seyferth and Henk 2006). The kinetic energy in PFC2d is dissipated through two mechanisms: (a) plastic or frictional yielding; and (b) damping. Damping in PFC2D works on the acceleration motion rather than velocity and is considered as local and non-viscous with the advantage of not inhibiting steady motion (Itasca 1999, Seyferth and Henk 2006).

3. Methods

3.1 Point load test method

The testing procedure and standard suggested by ASTM (2002) is used for determining Is(50) with the following equation for the index

$$I_S(50) = F\left(\frac{P}{D_e^2}\right) \tag{1}$$

Where P is the peak load, De is the equivalent core diameter, and F is the size correction factor, $(De/50)^{0.45}$ (see Fig. 1(a)).

3.2 Brazilian test method

The Brazilian test is suggested by the International Society for Rock Mechanics (ISRM 1978) and is conducted for determining the tensile strength of material, σ_t, with the following equation

$$\sigma_t = \frac{2P}{\pi Dt} \tag{2}$$

Where P is the peak load, D is the core diameter, and t is

Table 1 Micro properties used to represent the model with tensile strength of 4.6 MPa

Property	Value	Property	Value
Type of particle	disc	Parallel bond radius muliplier	1.4
Densiy (kg/m^3)	3000	Youngs modulus of parallel bond (GPa)	1.7
Minimum radius (mm)	0.27	Parallel bond stifness ratio (pb_kn/pb_ks)	3
Size ratio	1.56	Particle friction coefficien	0.5
Porosity ratio	0.08	Parallel normal strength, mean (MPa)	50
Local damping coefficient	0.7	Parallel normal strength, std. dev (MPa)	5
Contact young modulus (GPa)	12	Parallel shear strength, mean (MPa)	50
Stiffness ratio (kn/ks)	1.7	Parallel shear strength, std. dev (MPa)	5

(a)

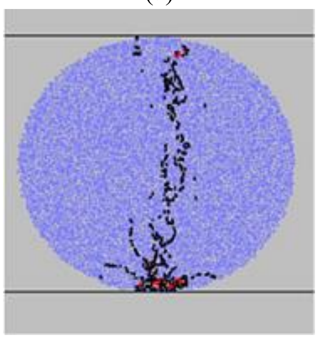

(b)

Fig. 2 Failure pattern in (a) tested specimen and (b) PFC2D model

the specimen thickness. (See Fig. 1(b)).

4. Preparations and calibration of the PFC2D model

The standard process of generation of a PFC2D assembly to represent a test model involves four steps: (a) particle generation and packing the particles, (b) isotropic stress application, (c) floating particle elimination, and (d) bond installation. The following section describes how the Brazilian tests in the laboratory were used for the calibration of the PFC2D models.

4.1 PFC2D calibration using Brazilian tests

Brazilian tests were used to calibrate the tensile strength of three different models in PFC2D. Adopting the micro-properties listed in Table 1 with the standard calibration

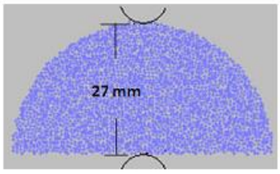

(a)

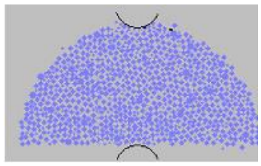

(b)

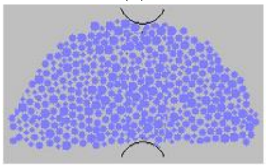

(c)

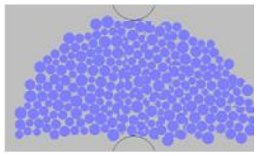

(d)

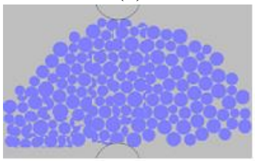

(e)

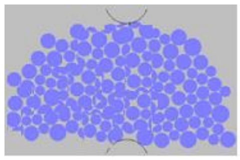

(f)

Fig. 3 Semi-circular models with same diameter (54 mm) and mean particle diameter of (a) 0.27 mm, (b) 0.47 mm, (c) 0.67 mm, (d) 0.87 mm, (e) 1.07 mm and (f) 1.27 mm

procedures (Potyondy and Cundall 2004), three calibrated PFC particle assembly were created. These parameters obtained by try and error approach which explain in detail by Itasca 1999. The diameter of the Brazilian disk considered in the numerical tests was 54 mm. The specimens were made of 5,615 particles with different clump particle distributed in it to gain the best results. The disk was crushed by the lateral walls moved toward each other with a low speed of 0.016 m/s. Fig. 2(a), (b) illustrates the failure pattern of the numerical and experimental tested specimens, respectively. A great agreement between the results of numerical models and the experiments can be seen in Fig. 2. Interestingly, the values of normal stress resulting in the fracturing of specimens were 1 MPa and 1.1 MPa for laboratory experiment and PFC2D, respectively.

4.2 Numerical simulations of point load and Brazilian tests

4.2.1 Preparing the model

After calibration of PFC2D, point load test was simulated by creating the semi-circular models (Figs. 3-4). Six models with the diameter of 54 mm and with different mean particle sizes of 0.27 mm, 0.47 mm, 0.67 mm, 0.87 mm, 1.07 mm, and 1.27 mm were prepared (Fig. 3). In addition, to evaluate the effect of specimen diameter, four models with the particle size of 0.27 mm and diameters of 75 mm, 54 mm, 25 mm and 12.5 mm were studies (Fig. 4). The vertical distance between the two loading walls in models with diameters of 75 mm, 54 mm, 25 mm and 12.5 mm was fixed at 75 mm, 54 mm, 25 mm and 12.5 mm, respectively.

Brazilian tests were also simulated by creating circular models as shown in Figs. 5-6. Similar to the models made in semi-circular geometry, Brazilian test models were

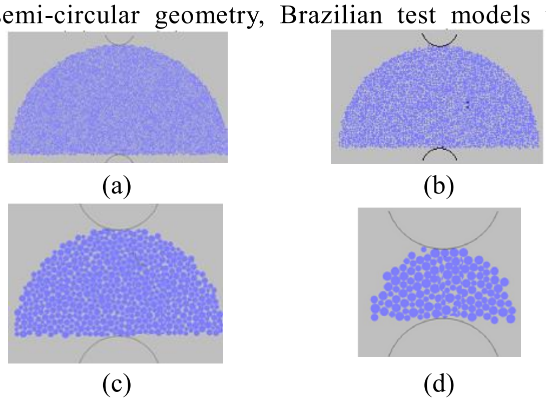

Fig. 4 Semi-circular models with same mean particle diameter of 0.27 mm and diameters of (a) 75 mm, (b) 54 mm, (c) 25 mm, and (d) 12.5 mm

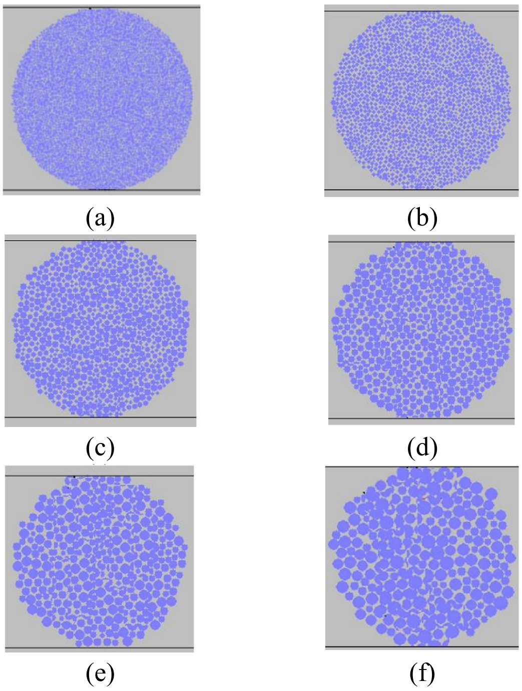

Fig. 5 Circular models with same diameter of 54 mm and mean particle size of (a) 0.27 mm, (b) 0.47 mm, (c) 0.67 mm, (d) 0.87 mm, (e) 1.07 mm and (f) 1.27 mm

prepared with the following dimensions: (a) diameter of 54 mm and the mean particle size of 0.27 mm, 0.47 mm, 0.67 mm, 0.87 mm, 1.07 mm, and 1.27 mm (Fig. 5); and (b) particle size of 0.27 mm and the diameters of 75 mm, 54 mm, 25 mm, and 12.5 mm (Fig. 6). Two loading walls were situated in the top and bottom of the specimens. The upper wall was moved in Y direction and the lower wall in the opposite Y direction with the low speed of 0.016 m/s.

4.2.2 Failure mechanisms in numerical models

(a) Point Load Tests

Fig. 7(a)-(f) shows the progress of cracks in the semi-circular models with the different mean particle sizes. The black and red lines indicate the tensile and shear cracks, respectively. It is clear that the tensile cracks are dominant mode of failure for all models. The cracks propagate in a more linear and disconnected path as the mean particle size

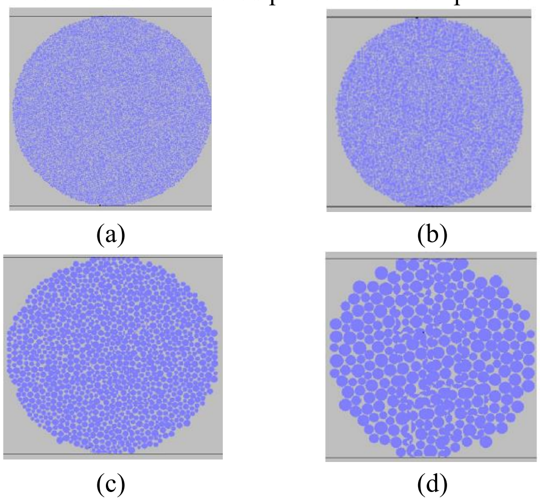

Fig. 6 Circular models with same mean particle diameter of 0.27 mm and diameter of (a) 75mm, (b) 54 mm, (c) 25 mm, and (d) 12.5 mm

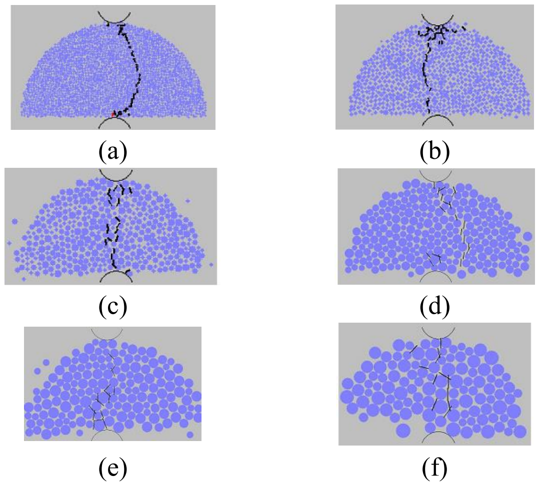

Fig. 7 Failure pattern in semi-circular models with mean particle diameter of (a) 0.27 mm, (b) 0.47mm, (c) 0.67 mm, (d) 0.87 mm, (e) 1.07 mm and (f) 1.27 mm; diameter of all models is 54 mm

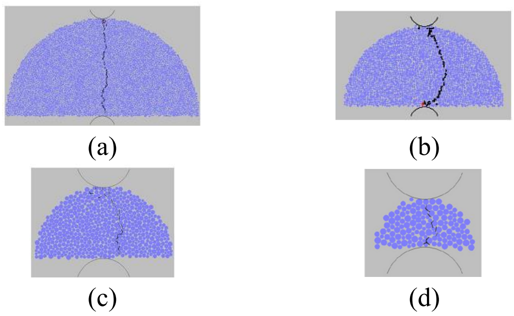

Fig. 8 Failure pattern in semi-circular models with diameter of (a) 75 mm, (b) 54 mm, (c) 25 mm, (d) 12.5 mm. The mean particle size for all models was 0.27 mm

increases. Fig. 8(a)-(d) shows the progress of cracks in semi-circular models with diameter of 75 mm, 50 mm, 25 mm and 12.5 mm, respectively. Black line and red line represent tensile cracks and shear cracks, respectively. In these models, also the tensile cracks were the dominant mode of failure and the failure pattern was the same for all models. In other word, for the constant particle size models, the model dimension does not have a strong influence on the failure pattern.

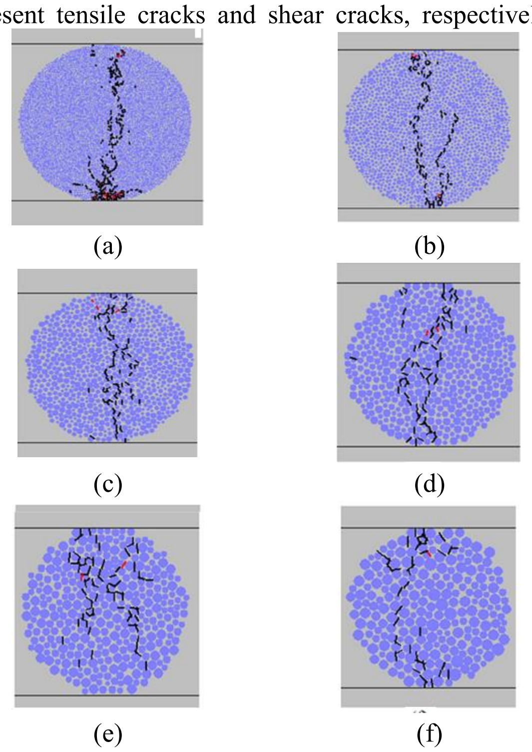

Fig. 9 Failure pattern in the circular models with the mean particle diameter of (a) 0.27 mm, (b) 0.47 mm, (c) 0.67 mm, (d) 0.87 mm, (e) 1.07 mm and (f) 1.27 mm. All models had the diameter of 54 mm

b) Brazilian test

Fig. 9(a)-(f) shows the progress of cracks in the circular models with the mean particle sizes of 0.27 mm, 0.47 mm, 0.67 mm, 0.87 mm, 1.07 mm, and 1.27 mm, respectively. The black and red lines indicate the tensile and shear cracks, respectively. Tensile cracks are dominant mode of failure in all models and the shear bands (cracks) were reduced as the mean particle size increased. It is very obvious that the particle size has a large influence on the shape and accuracy of the cracking pattern.

Fig. 10(a)-(d) shows the progress of cracks in circular models with diameter of 75 mm, 50 mm, 25 mm and 12.5 mm, respectively. The failure pattern is nearly constant for all models and indicates that the model diameter does not influence the failure pattern.

4.2.3 The effect of model scale and particle size on Is(50)

Is(50) was measured using Eq. (1) for all models. Fig. 11(a) shows the effect of semi-circular models radius on the Is(50) while the mean particle size was constant. For models with the constant particle size, the Is(50) increased with increasing the radius of semi-circular models. Fig. 11(b) shows the effect of particle size on the Is(50) while model scale was constant. In this case, the Is(50) values increased with increasing the radius of models.

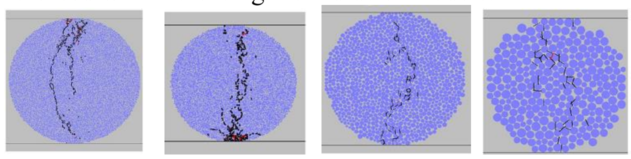

(a) (b) (c) (d)

Fig. 10 Failure pattern in circular models with diameter of (a) 75 mm, (b) 54 mm, (c) 25 mm, and (d) 12.5 mm. The particle diameter in all models was 0.27 mm

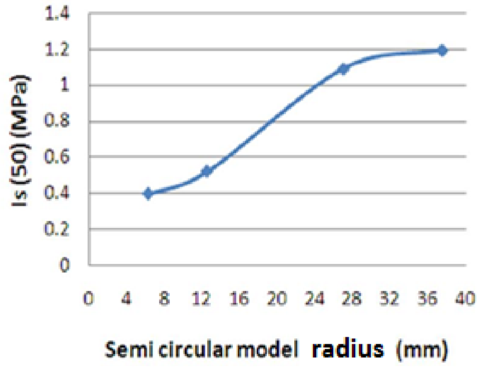

(a)

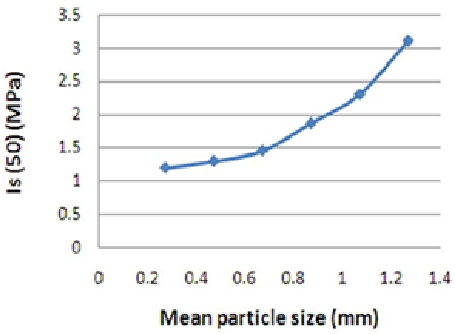

(b)

Fig. 11(a) the effect of radius of semi-circular models on the Is(50) and (b) the effect of particle size on the Is(50)

4.2.4 The effect of model scale and particle size on Brazilian tensile strength

Brazilian tensile strength values were measured using Eq. (2) for all models. Fig. 12(a) shows the effect of model radius on the Brazilian tensile strength while particle size was constant. For models with a constant particle size, the Brazilian tensile strength values increased with increasing the radius of models. Fig. 12(b) shows the effect of particle size on the Brazilian tensile strength while model scale is constant. In constant model scale, the Brazilian tensile strength increased with increasing the radius of models.

4.2.5 Relationship between Is(50) and tensile strength

Fig. 13(a) shows the variation of the ratio of tensile strength to Is(50) with the mean particle size. The ratio of tensile strength to Is(50) decreases as the mean particle size increases. The curve fitting equation shows that the ratio of tensile strength to Is(50)=-1.803*(mean particle size)^2+0.636 (mean particle size)+4.659. In other word, the tensile strength of models with each particle size can be calculated using above equation.

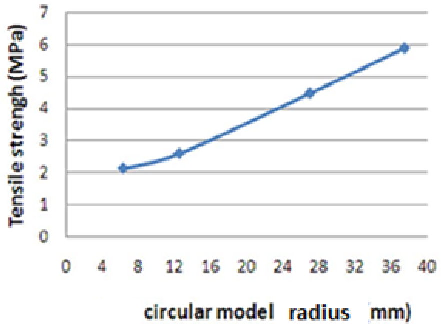

(a)

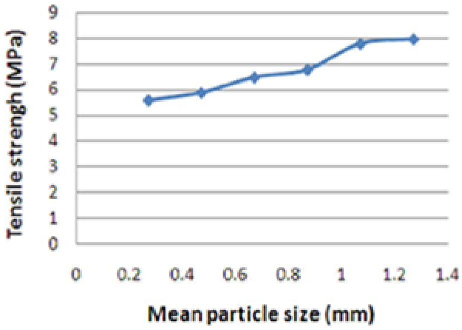

(b)

Fig. 12(a) the effect of radius of Brazilian models on the tensile strength and (b) the effect of particle size on the tensile strength

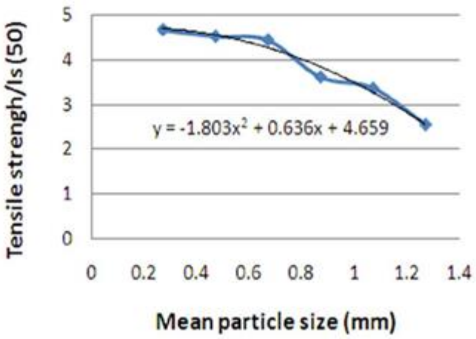

(a)

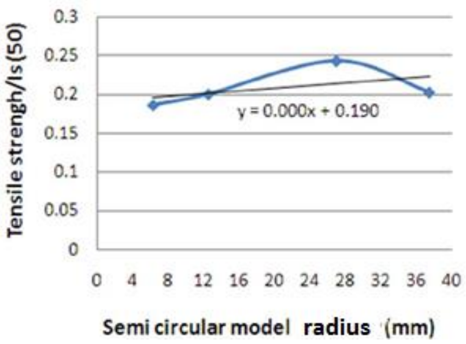

(b)

Fig. 13(a) variation of the ratio of Is(50) to tensile strength with mean particle size and (b) variation of the ratio of tensile strength to Is(50) with radius of semi-circular models

Fig. 13(b) shows variation of the ratio of tensile strength to Is(50) with diameter of semi-circular/Brazilian models. The ratio of tensile strength to Is(50) is nearly constant by increasing the model diameter. The curve fitting equation shows that the ratio of tensile strength to Is(50) of 0.19. In other word, the tensile strength of models with different model diameter is roughly about 0.19 times the tensile strength values.

5. Results

In this study, the effects of model scale and particle size on point load index, tensile strength and failure processes were investigated using the PFC2D numerical models. For this purpose, circular and semi-circular models with same particle size of 0.27 mm, and different model diameters of 75 mm, 54 mm, 25 mm and 12.5 mm were prepared. Also, circular and semi-circular models with diameter of 27 mm and different particle sizes of 0.27 mm, 0.47 mm, 0.67 mm, 0.87 mm, 1.07 mm and 1.27 mm were simulated using PFC2D and tested under both point load and Brazilian configurations. The results of numerical simulations show the failure pattern is not very sensitive to the model scale but it is very sensitive to the mean particle size. Both Is(50) and Brazilian tensile strength values showed an increase with the increase in the model diameter and particle size. The ratio of Brazilian tensile strength to Is(50) decreased as the particle size increased but was nearly constant as the model scale increased. It's to be note that the limitations of DEM is (a) Fracture is closely related to the size of elements, and that is so called size effect. (b) Cross effect exists because of the difference between the size and shape of elements with real grains. (c) In order to establish the relationship between the local and macroscopic constitutive laws, data obtained from classical geomechanical tests which may be impractical are used (Donze *et al.* 2009).

References

Al-Busaidi, A., Hazzard, J.F. and Young, R.P. (2005), "Distinct element modeling of hydraulically fractured lac du bonnet granite", *J. Geophys. Res.*, **110**, B06302.

Aoki, K., Mito, Y. and Mori, T. *Evaluation of Behavior of EDZ around Rock Cavern by AE Measurements and DEM Simulation Using Bonded Particle Model.*

ASTM (2002), *Standard Test Method for Determination of the Point Load Strength Index of Rock*, Am Soc Test Mater, ASTM D 5731-02.

Bahaaddini, M., Hagan, P.C., Mitra, R. and Hebblewhite, B.K. (2014), "Parametric study of smooth joint parameters on the shear behaviour of rock joints", *Rock Mech. Rock. Eng.*, **48**(3), 923-940.

Bahaaddini, M., Sharrock, G. and Hebblewhite, B.K. (2013a), "Numerical direct shear tests to model the shear behaviour of rock joints", *Comput. Geotech.*, **51**, 101-115.

Bahaaddini, M., Sharrock, G. and Hebblewhite, B.K. (2013b), "Numerical investigation of the effect of joint geometrical parameters on the mechanical properties of a non-persistent jointed rock mass under uniaxial compression", *Comput. Geotech.*, **49**, 206-225.

Bi, J., Zhou, X.P. and Qian, Q.H. (2016), "The 3D numerical

simulation for the propagation process of multiple pre-existing flaws in rock-like materials subjected to biaxial compressive loads", *Rock Mech. Rock Eng.*, **49**(5), 1611-1627.
Bi, J., Zhou, X.P. and Xu, X.M. (2017), "Numerical simulation of failure process of rock-like materials subjected to impact loads", *Int. J. Geomech.*, **17**(3), 04016073.
Burbidge, D.R. and Braun, J. (2002), "Numerical models of the evolution of accretionary wedges and fold-and-thrust belts using the distinct-element method", *Geophys. J. Int.*, **148**(3), 542-561.
Chiu, C.C., Wang, T.T., Weng, M.C. and Huang, T.H. (2013), "Modeling the anisotropic behavior of jointed rock mass using a modify ed smooth-joint model", *Int. J. Rock Mech. Min. Sci.*, **62**, 14-22.
Cundall, P.A. (1971), "A computer model for simulating progressive large scale movements in blocky rock systems", *Proceedings of the Symposium of the International Society for Rock Mechanics*, Nancy, France.
Cundall, P.A. (2001), *Numerical Experiments on Rough Joints in Shear Using a Bonded Particle Model*, In: Lehner FK, Urai JL, editors. Aspects of tectonic faulting (Festschrift in Honour of George Mandl), Springer, Berlin, Germany.
Cundall, P.A. (2011), "The synthetic rock mass approach for jointed rock mass modelling", *Int. J. Rock Mech. Min. Sci.*, **48**(2), 219-244.
Cundall, P.A. and Strack, O.D.L. (1979), "A discrete numerical model for granular assemblies", *Geotech.*, **29**(1), 47-65.
Dalguer, L.A., Ikikura, K. and Riera, J.D. (2003), "Generation of new cracks accompanied by the dynamic shear rupture propagation of the 2000 Tottori (Japan) earthquake", *Bull Seismol. Soc. Am.*, **93**(5), 2236-2252.
Donze, F.V., Richefeu, V. and Magnier, S.A. (2009), "Advances in discrete element method applied to soil rock and concrete mechanics", *Electr. J. Geolo. Eng.*, **8**(1), 1-44.
Erickson, S.G., Strayer, L.M. and Suppe, J. (2001), "Initiation and reactivation of faults during movement over a thrust-fault ramp: Numerical mechanical models", *J. Struct. Geol.*, **23**(1), 11-23.
Esmaieli, K., Hadjigeorgiou, J. and Grenon, M. (2010), "Estimating geometrical and mechanical REV based on synthetic rock mass models at Brunswick mine", *Int. J. Rock Mech. Min. Sci.*, **47**(6), 915-926.
Fakhimi, A., Carvalho, F., Ishida, T. and Labuz, J.F. (2002), "Simulation of failure around a circular opening in rock", *Int. J. Rock Mech. Min. Sci.*, **39**(4), 507-515.
Fan, X., Kulatilake, P.H.S.W. and Chen, X. (2015), "Mechanical behavior of rock-like jointed blocks with multi-non-persistent joints under uniaxial loading: A particle mechanics approach", *Eng. Geol.*, **190**, 17-32.
Ghazvinian, A., Sarfarazi, V., Schubert, W. and Blumel, M. (2012), "A study of the failure mech- anism of planar non-persistent open joints using PFC2D", *Rock Mech. Rock Eng.*, **45**(5), 677-693.
Hadjigeorgiou, J., Esmaieli, K. and Grenon, M. (2009), "Stability analysis of vertical excavations in hard rock by integrating a fracture system into a PFC model", *Tunn. Undergr. Sp. Tech.*, **24**(3), 296-230.
Haeri, H. (2015a), "Propagation mechanism of neighboring cracks in rock-like cylindrical specimens under uniaxial compression", *J. Min. Sci.*, **51**(3), 487-496.
Haeri, H. (2015b), "Influence of the inclined edge notches on the shear-fracture behavior in edge-notched beam specimens", *Comput. Concrete*, **16**(4), 605-623.
Haeri, H. (2016), "Propagation mechanism of neighboring cracks in rock-like cylindrical specimens under uniaxial compression", *J. Min. Sci.*, **51**(5), 1062-1106.
Haeri, H. and Sarfarazi, V. (2016a), "The effect of non-persistent joints on sliding direction of rock slopes", *Comput. Concrete*, **17**(6),723-737.
Haeri, H., Khaloo, A. and Marji, M.F. (2015), "Experimental and numerical simulation of the microcrack coalescence mechanism in rock-like materials", *Strength Mater.*, **47**(5), 740-754.
Haeri, H., Sarfarazi, V. and Hedayat, A. (2016), "Suggesting a new testing device for determination of tensile strength of concrete", *Struct. Eng. Mech.*, **60**(6), 939-952.
Haeri, H., Sarfarazi, V. and Lazemi, H.A. (2016b), "Experimental study of shear behavior of planar non-persistent joint", *Comput. Concrete*, **17**(5), 639-653.
Haeri, H., Sarfarazi, V., Bagher Shemirani, A.R. and Hosseini, S.S. (2017), "Experimental and numerical investigation of the effect of sample shapes on point load index", *Geomech. Eng.*, **13**(6), 1045-1055.
Haeri, H., Shahriar, K. and Marji, M.F. (2013), "Modeling the propagation mechanism of two random micro cracks in rock samples under uniform tensile loading", *Proceedings of the ICF13*.
Hazzard, J.F. and Young, R.P. (2000), "Simulating acoustic emissions in bonded-particle models of rock", *Int. J. Rock Mech. Min. Sci.*, **37**(5), 867-872.
Hazzard, J.F. and Young, R.P. (2004), "Dynamic modelling of induced seismicity", *Int. J. Rock Mech. Min. Sci.*, **41**(8), 1365-1376.
ISRM, International Society for Rock Mechanics (1978), "Commission on standardization of laboratory and field tests. Suggested methods for determining tensile strength of rock materials", *Int. J. Rock Mech. Min. Sci. Geomech. Abstr.*, **15**, 99-103.
Itasca (1999), *PFC2D-Particle Flow Code in 2 Dimensions. Theory and Background*, Itasca Consulting Group, Minneapolis, U.S.A.
Konietzky, H. *Numerical Modeling in Micromechanics via Particle Methods*, Swets & Zeitlinger, Lisse, 269-276.
Lambert, C. and Coll, C. (2014), "Discrete modeling of rock joints with a smooth-joint contact model", *J. Rock Mech. Geotech. Eng.*, **6**(1), 1-12.
Li, J.Y., Zhou, H., Zhu, W. and Li, S. (2016), "Experimental and numerical investigations on the shear behavior of a jointed rock mass", *Geosci. J.*, **20**(3), 371-379.
Li, S., Wang, H., Li, Y., Li, Q., Zhang, B. and Zhu, H. (2016), "A new mini-grating absolute displacement measuring system for static and dynamic geomechanical model tests", *Measure.*, **82**, 421-431.
Li, Y., Zhou, H., Zhu, W., Li, S. and Liu, J. (2015), "Numerical study on crack propagation in brittle jointed rock mass influenced by fracture water pressure", *Mater.*, **8**(6), 3364-3376.
Mas Ivars, D., Pierce, M.E., Darcel, C., Reyes-Montes, J., Potyondy, D.O., Paul Young, R., Mora, P. and Place, D. (1993), "A lattice solid model for the nonlinear dynamics of earthquakes", *Int. J. Mod. Phys.*, **C4**, 1059-1074.
Mora, P. and Place, D. (1998), "Numerical simulation of earthquake faults with gouge: Toward a comprehensive explanation for the heat flow paradox", *J. Geophys. Res.*, **103**(B9), 21067-21089.
Morgan, J.K. and Boettcher, M.S. (1999), "Numerical simulations of granular shear zones using the distinct element method-1. Shear zone kinematics and the micromechanics of localization", *J. Geophys. Res.*, **104**(B2), 2703-2719.
Ohnishi, Y. and Aoki, K. (2004), "Contribution of rock mechanics to the new century", *Proceedings of the 3rd Asian Rock Mechanics Symposium*, Mill Press, Rotterdam. the Netherlands.
Okabe, T., Haba, T., Mitarashi, Y., Tezuka, H. and Jiang, Y. (2004), "Study on the effect of tunnel face stabilization using the distinct element method", *Proceedings of the 3rd Asian Rock Mechanics Symposium*, Mill Press, Rotterdam, the Netherlands.
Park, E.S., Martin, C.D. and Christiansson, R. (2004), "Simulation of the mechanical behavior of discontinuous rock masses using a bonded-particle model", *Proceedings of the 6th North*

America Rock Mechanics Symposium (NARMS), Houston, Texas, U.S.A.

Potyondy, D.O. and Cundall, P.A. (2004), "A bonded-particle model for rock", *Int. J. Rock Mech. Min. Sci.*, **41**(8), 1329e64.

Sainsbury, D.P., Cai, Y. and Hebblewhite, B.K. (2003), *Numerical Investigation of Crown Pillar Recovery Beneath Stabilized Rockfill*, In: Konietzky, H. (ed) Numerical Modeling in Micromechanics via Particle Methods, Swets & Zeitlinger, Lisse, the Netherlands, 225-231.

Sardemir, M. (2016), "Empirical modeling of flexural and splitting tensile strengths of concrete containing fly ash by GEP", *Comput. Concrete*, **17**(4), 489-498.

Sarfarazi, V., Faridi, H.R., Haeri, H. and Schubert, W. (2016a), "A new approach for measurement of anisotropic tensile strength of concrete", *Adv. Concrete Constr.*, **3**(4), 269-284.

Sarfarazi, V., Haeri, H. and Khaloo, A. (2016b), "The effect of non-persistent joints on sliding direction of rock slopes", *Comput. Concrete*, **17**(6), 723-737.

Scholtès, L. and Donzé, F.V. (2012), "Modelling progressive failure in fractured rock masses using a 3D discrete element method", *Int. J. Rock Mech. Min. Sci.*, **52**, 18-30.

Scott, D.R. (1996), "Seismicity and stress rotation in a granular model of the brittle crust", *Nat.*, **381**, 592-595.

Seyferth, M. and Henk, A. (2002), "Coupled DEM and FEM models: An approach to bridge the gap between large-scale geodynamic and high-resolution tectonic modeling", *EOS Trans.*, **83**, 1376-1377.

Seyferth, M. and Henk, A. (2006), "A numerical sandbox: High-resolution distinct element models of halfgraben formation", *Int. J. Earth Sci.*, **95**(2), 189-203.

Shaowei, H., Aiqing, X., Xin, H. and Yangyang, Y. (2016), "Study on fracture characteristics of reinforced concrete wedge splitting tests", *Comput. Concrete*, **18**(3), 337-354.

Shuraim, A.B., Aslam, F., Hussain, R. and Alhozaimy, A. (2016), "Analysis of punching shear in high strength RC panels-experiments, comparison with codes and FEM results", *Comput. Concrete*, **17**(6), 739-760.

Silling, S.A. (2000), "Reformulation of elasticity theory for discontinuities and long-range forces", *J. Mech. Phys. Sol.*, **48**(1), 175-209.

Strayer, L.M. and Suppe, J. (2002), "Out-of-plane motion of a thrust sheet during along-strike propagation of a thrust ramp: A distinct-element approach", *J. Struct. Geol.*, **24**(4), 637-650.

Tannant, D.D. and Wang, C. (2004), "Thin tunnel liners modeled with particle flow code", *Eng. Comput.*, **21**(2/3/4), 318-342.

Van Vliet, M.R.A. and Van Mier, J.G.M. (2000), "Experimental investigation of size effect in concrete and sandstone under uniaxial tension", *Eng. Fract. Mech.*, **65**(2-3), 165-188.

Vietor, T. (2003), *Numerical Simulation of Collisional Orogeny Using the Distinct Element Technique*, In: Konietzky H (ed) Numerical Modeling in Micromechanics via Particle Methods, Swets & Zeitlinger, Lisse, the Netherlands, 295-301.

Vorechovsky, M. (2007), "Interplay of size effects in concrete specimens under tension studied via computational stochastic fracture mechanics", *Int. J. Sol. Struct.*, **44**(9), 2715-2731.

Wang, C., Tannant, D.D. and Lilly, P.A. (2003), "Numerical analysis of the stability of heavily jointed rock slopes using PFC2D", *Int. J. Rock Mech. Min. Sci.*, **40**(3), 415-424.

Wang, C., Tannant, D.D. and Lilly, P.A. (2003), "Numerical analysis of the stability of heavily jointed rock slopes using PFC2D", *Int. J. Rock Mech. Min. Sci.*, **40**(3), 415-424.

Wang, X., Zhu, Z., Wang, M., Ying, P., Zhou, L. and Dong, Y. (2017), "Study of rock dynamic fracture toughness by using VB-SCSC specimens under medium-low speed impacts", *Eng. Fract. Mech.*, **181**, 52-64.

Xu, L. and Ren, Q. (2014), "Particle flow simulation of direct shear test of rock discontinuities", *Adv. Mater. Res.*, **1065-1069**, 159-163.

Yang, S.Q. (2015), "An experimental study on fracture coalescence characteristics of brittle sandstone specimens combined various flaws", *Geomech. Eng.*, **8**(4), 541-557.

Yi, S., Wang, G.F. and Zhou, Q.H. (2014), "Tunnel face stability and ground settlement in pressurized shield tunneling", *J. Centr. South Univ.*, **21**(4), 1600-1606.

Zhao, H.H., Shao, L.T. and Ji, S.Y. (2011), *Numerical Simulation of Triaxial Test on the Dense Sand by DEM*, Geotechnical Special Publication No. 222, ASCE, 233 Instrumentation.

Zhou, X.P. and Yang, H.Q. (2012), "Multiscale numerical modeling of propagation and coalescence of multiple cracks in rock masses", *Int. J. Rock Mech. Min. Sci.*, **55**, 15-27.

Zhou, X.P., Bi, J. and Qian, Q.H. (2015), "Numerical simulation of crack growth and coalescence in rock-like materials containing multiple pre-existing flaws", *Rock Mech. Rock Eng.*, **48**(3), 1097-1114.

Zhou, X.P., Gu, X.B. and Yang, Y.T. (2015), "Numerical simulations of propagation, bifurcation and coalescence of cracks in rocks", *Int. J. Rock Mech. Min. Sci.*, **80**, 241-254.

Zi, G., Kim, J. and Bazant, Z.P. (2014), "Size effect on biaxial flexural strength of concrete", *ACI Mater. J.*, **111**(3), 1-8.

CC